Throughput equalization in mean-field hard-core models for CSMA-based wireless networks

Toshiyuki Tanaka
Graduate School of Informatics
Kyoto University
Yoshida Hon-machi, Sakyo-ku
Kyoto, 606-8501 Japan
Email: tt@i.kyoto-u.ac.jp

Shashi Prabh
School of Engineering
Shiv Nadar University
Dadri, UP 201314. India
Email: shashi.prabh@snu.edu.in

Yiyan Liu
Graduate School of Informatics
Kyoto University
Yoshida Hon-machi, Sakyo-ku
Kyoto, 606-8501 Japan
Email: lau@sys.i.kyoto-u.ac.jp

***Abstract*—In this paper we consider the problem of equalizing throughput of nodes in CSMA-based wireless networks. We model interference in a network using conflict graph, where edges represent hard-core interaction, meaning that the two nodes an edge connects cannot be simultaneously active, or transmitting. In practice, the degrees of nodes in a conflict graph are not constant. In such cases, using CSMA leads to lack of fairness since nodes with larger degree have the potential of getting hold of the medium for smaller fraction of time than the nodes with smaller degree. We present a distributed strategy for throughput equalization. The proposed strategy is based on a mean-field hard-core model of interference, and it equalizes the throughput of the nodes with different degrees. We also show that the mean-field hard-core model exhibits a certain phase transition. We present results of Monte-Carlo simulations to evaluate the the proposed strategy in square grid networks and Poisson networks, in addition to mean-field networks.**

I. Introduction

Carrier Sense Multiple Access with collision avoidance (CSMA/CA) is a widely used medium access control (MAC) protocol in wireless ad-hoc networks. In CSMA-based networks, nodes perform carrier sensing before initiating a transmission, and continue on to transmit only if the medium is free. Medium is considered to be free if carrier sensing returns a value below some specified threshold. If the transmitter senses the medium to be busy, it starts a backs-off timer. Upon the expiration of the timer, it repeats the process starting with carrier sensing once again. In practice, the method used for setting back-off timers is somewhat more elaborate and can be found in standard networking textbooks [1], [2]. Although CSMA is somewhat old [3], there has been renewed interest in the analysis of CSMA, primarily because of recent research results, but also due to the development of new wireless systems using CSMA, such as cognitive radio.

Various lines of approach exist for statistical modeling of the blocking of nodes due to interference. Stochastic geometry [4] offers one such approach where spatial point processes are used to model the locations of wireless nodes [5], [6]. In this context, Matérn hard-core point processes (HCPP) [7], which are defined on the basis of Poisson point processes (PPPs), have been studied extensively. Matérn type I process is defined as follows. First a set of points in $\mathbb{R}^n$ are generated using homogeneous PPP, followed by eliminating some of the points in order to have no point within distance less than the hard-core distance δ of any remaining point. Matérn type II process is a dynamical version of Matérn type I process where points in $\mathbb{R}^n$ are generated sequentially according to a PPP while discarding all the points that fall within distance δ of the points generated earlier. Thus, the occurrence of interference is determined geometrically using the distance δ as "interference range." Some results on the analysis of interference using HCPP exist in [8], [9], [10], [11], [12].

In this paper we take another approach, namely, that of mean-field modeling as used in the context of statistical mechanics of spin glasses applied to computational and information theoretic problems [13], [14]. In this context, by mean-field models we mean models that do not consider the geometrical structure, something that is present in models defined on finite-dimensional spaces. These models can also be referred as Gilbert's random graph model $G(n, p)$ [15]. We shall, however, use the term mean-field to maintain the convention adopted in the previous literature the results of which we have used in this work. In scattering-rich environments the distance between two nodes is no longer the determining factor for the strength of interference between them. One may argue that the complete disregard for the geometrical structure in the mean-field modeling would be justifiable to some extent in such environments. Moreover, simulation data presented here suggest that the effectiveness of the equalization strategy derived using this model carries over to geometric models.

In the following, we represent interference in a network by a conflict graph where an edge represents hard-core interaction, that is, the two nodes it connects cannot be simultaneously active. In general the node degrees will vary. This leads to lack of fairness in the sense that nodes with larger degree have the potential of getting hold of the medium for smaller fraction of time as compared to nodes with smaller degree. Lack of fairness in a medium access protocol is generally considered harmful since it can cause starvation and bottlenecks. We present a distributed strategy for throughput equalization in CSMA wireless networks, backed by a rigorous theory of mean-field hard-core model of interference. The results of this work are particularly applicable to large networks, e.g., large-scale wireless sensor networks or highly dense networks [16].

II. Model and analysis

A. Mean-field hard-core models

In this section, we introduce a mean-field hard-core model of interference. This is followed by the motivation, discussed in Section II-B, for using belief propagation in this work.

Let $G = (V, E)$ be a graph where V denotes the set of nodes and $E \subset V \times V$ the set of edges. A hard-core model on the graph G is defined by regarding G as a conflict graph: Each element of V represents a wireless node whose state can be either active or inactive. An edge implies that the two nodes it connects have hard-core interaction so that they cannot be simultaneously active. Let $\boldsymbol{s} = (s_1, \ldots, s_{|V|}) \in \{0, 1\}^{|V|}$ be a vector representing the states of the nodes in G, with $s_i = 1$ and 0 representing that node i is active and inactive, respectively.

The hard-core model we study in this paper is defined in terms of the probability distribution of the state vector $\boldsymbol{s}$, as

$$p(\boldsymbol{s}; \boldsymbol{\mu}) = \frac{1}{Z} \prod_{i \in V} e^{\mu_i s_i} \prod_{(ij) \in E} (1 - s_i s_j), \tag{1}$$

where $\boldsymbol{\mu} = (\mu_1, \ldots, \mu_{|V|}) \in \mathbb{R}^{|V|}$ wherein μ_i controls the average activity (defined below (2)) of node i, and Z is the partition function. More precisely, the parameter μ_i defines the average activity of node i with hard-core interactions absent as $e^{\mu_i}/(1+e^{\mu_i})$. One can think of this quantity as the fraction of time a node would remain busy transmitting if it was not limited by interference. In the context of statistical mechanics, the parameter μ_i corresponds to the chemical potential. In this paper, we call the parameter μ_i the intensity of node i.

Properties of the hard-core model (1) depend on the underlying graph G. In this paper we consider an ensemble of random graphs, and a conflict graph is assumed to be sampled from the random ensemble. A random ensemble is defined by first specifying a degree distribution $\{\lambda(d)\}_{d \in \{0,1,\ldots\}}$. Then for each $d \in \{0, 1, \ldots\}$, $n_d \approx |V|\lambda(d)$ nodes with degree d are prepared by adding d stubs. A set of edges, where $|E| = (|V|/2) \sum_d d\lambda(d)$ is also prepared. An instance of the random graph ensemble is generated by connecting the stubs with randomly chosen edges such that each edge connects exactly two different nodes. We call hard-core model defined on such a random graph ensemble mean-field hard-core model. As opposed to hard-core models defined on the basis of a spatial point process [8], [9], [10], [11], [12], the mean-field hard-core models completely ignore geometrical structure of the space in which nodes are distributed.

It should be noted that in our modeling we have assumed a saturated scenario, meaning that the queue of packets ready for transmission is never empty in all nodes. One might be able to consider the non-saturated scenario [17] in the mean-field hard-core models, which however, is beyond the scope of this paper.

B. Belief propagation and density evolution

Evaluating the mean activity of node i, defined as

$$\rho_i = \sum_{\boldsymbol{s}} s_i \, p(\boldsymbol{s}; \boldsymbol{\mu}), \tag{2}$$

is, in general, computationally hard. In fact, in the special case where $\boldsymbol{\mu} = \boldsymbol{0}$, the partition function normalizing the probability distribution (1) is equal to the number of independent sets in G, which is known to be #P-complete [18].In order to circumvent the computational difficulty, we consider the large-system limit, in which the number of nodes tends to infinity while the degree distribution λ is kept fixed. In the large-system limit a graph instance is asymptotically free of cycles of finite length. It motivates us to approximate mean activities by using belief propagation [19], where the results are expected to become exact in the large-system limit.

Application of belief propagation to the hard-core model (1) yields the following message update formula:

$$\pi_{i \to j} = \frac{e^{\mu_i} \prod_{k \in \partial i \backslash j} (1 - \pi_{k \to i})}{1 + e^{\mu_i} \prod_{k \in \partial i \backslash j} (1 - \pi_{k \to i})}, \quad (i, j) \in E, \tag{3}$$

where $\pi_{i \to j}$ denotes the message propagated from node i to node j, and where $\partial i \backslash j$ denotes the set of neighboring nodes of node i in G excluding node j.

If the graph G is cycle-free, then the messages converge after a finite number of message updates. The mean activity ρ_i of node i is then evaluated with the converged messages as

$$\rho_i = \frac{e^{\mu_i} \prod_{j \in \partial i} (1 - \pi_{j \to i})}{1 + e^{\mu_i} \prod_{j \in \partial i} (1 - \pi_{j \to i})}. \tag{4}$$

If the graph G has cycles, then there is in general no theoretical guarantee for the exactness of the above evaluation, nor even convergence of messages. Nonetheless, if the messages converge, one can apply (4) to obtain an approximation of mean activities.

In the large-system limit with a fixed degree distribution, the equilibrium of belief propagation can be macroscopically characterized via density evolution [20]. Since in the large-system limit, the underlying graph is asymptotically free of cycles of finite length, incoming messages $\{\pi_{k \to i}\}_{k \in \partial i \backslash j}$ can be regarded as independent samples from a message distribution $P(\pi)$. At equilibrium, the message updating (3) does not change the message distribution. This self-consistency condition can be represented in terms of the density evolution equation

$$P(\pi) = \mathbb{E}_{\mu, d} \left[\int \delta \left(\pi - \frac{e^{\mu} \prod_{k=1}^{d-1} (1 - \pi_k)}{1 + e^{\mu} \prod_{k=1}^{d-1} (1 - \pi_k)} \right) \times \prod_{k=1}^{d-1} (P(\pi_k) \, d\pi_k) \right], \tag{5}$$

where $\mathbb{E}_{\mu, d}$ denotes the average over the joint distribution of intensity μ and degree d of nodes. The message distribution $P(\pi)$ is obtained as a solution of the density evolution equation (5). The mean activity $\rho(\mu, d)$ of a node with intensity μ and degree d is then estimated on the basis of the message distribution $P(\pi)$ as

$$\rho(\mu, d) = \int \frac{e^{\mu} \prod_{k=1}^{d} (1 - \pi_k)}{1 + e^{\mu} \prod_{k=1}^{d} (1 - \pi_k)} \prod_{k=1}^{d} (P(\pi_k) \, d\pi_k). \tag{6}$$

Although in general one has to solve the density evolution equation (5) numerically, one can obtain an analytic solution in some special cases. A well known such case is where μ and d are constant across the whole network. In this case one has a solution of the form $P(\pi) = \delta(\pi - \bar{\pi})$, where $\bar{\pi}$ satisfies $\bar{\pi} = e^{\mu}(1-\bar{\pi})^d$. The estimated mean activities are independent of nodes, and are equal to

$$\rho = \frac{\bar{\pi}}{1+\bar{\pi}}. \tag{7}$$

III. Throughput equalization

In this section, we consider the problem of throughput equalization [21] in our mean-field hard-core model. The objective is to adjust $\boldsymbol{\mu}$ so as to equalize activities of the nodes.

Just as in the case where intensity and degree are constant, as discussed in the previous section, we assume that by appropriately choosing the degree-dependent intensities $\mu(d)$ the message distribution $P(\pi)$ becomes a delta function, that is, $P(\pi) = \delta(\pi - \bar{\pi})$. In order to satisfy the assumption, one has to define $\mu(d)$ so that the quantity

$$e^{\mu(d)}(1-\bar{\pi})^{d-1} \tag{8}$$

is independent of the degree d. Letting $a = e^{\mu(d)}(1-\bar{\pi})^{d-1}$, and on the basis of the assumption that the messages are all equal to $\bar{\pi}$, the belief propagation equation (3) can be written as

$$\bar{\pi} = \frac{a}{1+a}. \tag{9}$$

The estimated mean activity $\rho(d)$ of a node with degree d and intensity $\mu(d)$, obtained via belief propagation as in (4), is therefore given by

$$\rho(d) = \frac{e^{\mu(d)}(1-\bar{\pi})^d}{1+e^{\mu(d)}(1-\bar{\pi})^d} = \frac{\bar{\pi}}{1+\bar{\pi}}, \tag{10}$$

which is independent of the degree d, as expected. To the best of the authors' knowledge, this is a novel case where one can obtain an analytic solution to the mean-field hard-core model in the large-system limit.

Algorithm 1 Distributed throughput equalization strategy

Input: $\bar{\rho}$ ▷ Target activity, $0 < \bar{\rho} < 1/2$
Input: d ▷ Node degree, $d > 0$
1: $\mu(d) = \log\left((\bar{\rho}(1-\bar{\rho})^{d-1})/(1-2\bar{\rho})^d\right)$
2: $\rho_0(d) = e^{\mu(d)}/(1+e^{\mu(d)})$
Output: Transmit with probability $\rho_0(d)$

The above result leads to the throughput equalizing strategy described below and summarized in Algorithm 1. We require that mean activity of any node in the graph be equal to $\bar{\rho}$, that is, $\bar{\rho}$ is the specified target activity. From (10), one has $\bar{\pi} = \bar{\rho}/(1-\bar{\rho})$ and therefore

$$\mu(d) = \log\frac{\bar{\pi}}{(1-\bar{\pi})^d} = \log\frac{\bar{\rho}(1-\bar{\rho})^{d-1}}{(1-2\bar{\rho})^d}. \tag{11}$$

By fixing $\mu(d)$ in this way, equalization of the activities of the nodes is achieved. Hence Theorem 1 follows.

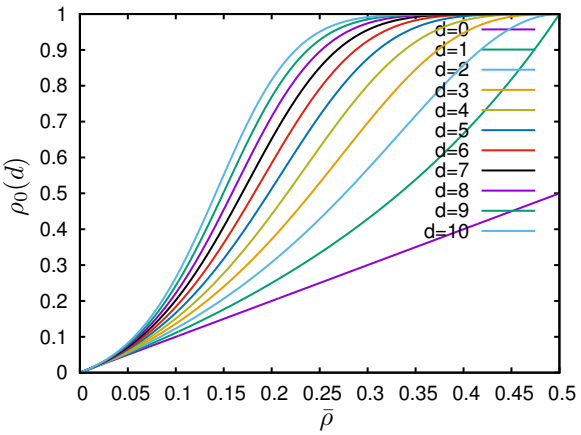

Fig. 1. $\rho_0(d)$ versus $\bar{\rho}$.

Theorem 1 (Throughput equaliztion)**.** *Let the average activity of a node (the intrinsic probability to use the channel in the absence of interference) of degree d be given by $\rho_0(d) = e^{\mu(d)}/(1+e^{\mu(d)})$. Then equalization of per-node throughput using CSMA is achieved in the mean-field hard-core model of interference by setting $\mu(d) = \log\left((\bar{\rho}(1-\bar{\rho})^{d-1})/(1-2\bar{\rho})^d\right)$, where $0 < \bar{\rho} < 1/2$ denotes the target equalized throughput.*

An interesting point is that the above throughput-equalizing strategy is local. The intensity of a node is determined by its own degree and does not depend on the degree distribution. A valid solution of (11) requires $\bar{\rho} < 1/2$ to hold. It should be noted that this is not a limitation since in non-trivial interference scenarios where degrees are greater than zero, achievable $\bar{\rho}$ cannot exceed 1/2.

The quantity

$$\rho_0(d) = \frac{e^{\mu(d)}}{1+e^{\mu(d)}} \tag{12}$$

represents the activity of a degree-d node with intensity $\mu(d)$ if the interference were absent. Figure 1 shows how $\rho_0(d)$ behaves as a function of $\bar{\rho}$. One can observe from this plot that nodes with a large degree should have a large value of $\rho_0(d)$ so as to compete against the large number of possible interferes.

The assumption of uniform-message solution $P(\pi) = \delta(\pi - \bar{\pi})$ is known to be invalid under certain conditions. A necessary condition for the uniform-message solution to be valid is local stability condition [22], which in our case corresponds to the local stability of belief propagation around the uniform-message solution $\pi_{i\to j} = \bar{\pi}$. Linearization of message update formula (3) around $\pi_{i\to j} = \bar{\pi}$ is given in terms of a Jacobian matrix that is equal to $-\bar{\pi}$ times the nonbacktracking matrix B of G [23], which is a $2|E| \times 2|E|$ matrix with elements defined as

$$B_{i\to j,k\to l} = \begin{cases} 1, & l = i,\ j \neq k \\ 0, & \text{otherwise} \end{cases}. \tag{13}$$

The local stability is therefore determined by the spectrum of B, and for the random graph ensemble used in this work, the

spectrum of B has been studied in [23]. Using their result, the stability condition is given by

$$c\bar{\pi}^2 < 1, \tag{14}$$

where

$$c = \frac{\sum_d d^2\lambda(d)}{\sum_d d\lambda(d)} - 1. \tag{15}$$

Hence Theorem 2 follows.

Theorem 2 (Stability of throughput equaliztion theorem)**.** *Let* $\bar{\pi} = \bar{\rho}/(1-\bar{\rho})$*. Then the stability region of Theorem 1 is given by* $c\bar{\pi}^2 < 1$ *where* c *is given by* (15)*.*

For a constant-degree ensemble, we get $c = d - 1$ where d is the degree, and the above local stability condition (14) is reduced to that in [22].

IV. Numerical experiments

A. Mean-field networks

Performing numerical experiments entailed generating instances of large random graphs with prescribed degree distributions. Some degree sequences, such as $\{3, 3, 1, 1\}$, cannot be realized in a simple graph. The degree sequences that are realizable in a simple graph are called graphical. Erdös-Gallai theorem can be used to test whether a degree sequence is graphical. Efficient linear time algorithms that use the theorem to verify graphicality exist in the literature [24], [25]. We observed that, apart form having wrong parity, degree sequences generated using uniform probability distribution for large number of nodes were almost always graphical. In the case of odd parity of the sequence, we simply select one of the elements of the sequence, say d_i, that can be increased or decreased without violating the degree distribution constraints (e.g., allowable as well as the minimum and the maximum degrees) and change the parity of d_i. Since the number of nodes is large, doing so does not affect the overall degree distribution. Once a graphical degree sequence of prescribed degree distribution is found, graphs realizing the sequence can be generated using methods proposed recently [26], [27]. For our numerical experiments we used the algorithms of [24], [26], as well as the code distributed by the authors of [27].

In the first set of numerical experiments a degree distribution λ was first specified, and a random graph instance with the specified degree distribution was generated. The intensities $\boldsymbol{\mu}$ were then determined via the analytical formula (11). We performed Monte-Carlo updates of the states of the nodes by randomly selecting a node and then stochastically updating its state taking into account the hard-core interactions. After a burn-in period, which was determined on the basis of temporal changes of network-wide average activities, we computed mean activities of the nodes in G. The total Monte-Carlo steps were set to $|V| \times 10^6$.

Figure 2 shows the results obtained for the case with $|V| = 5\,000$ and a few degree distributions, plotting the average $\overline{\rho(d)}$ as well as the variance of mean activities of nodes with degree d versus the target activity $\bar{\rho}$. We find that when the target

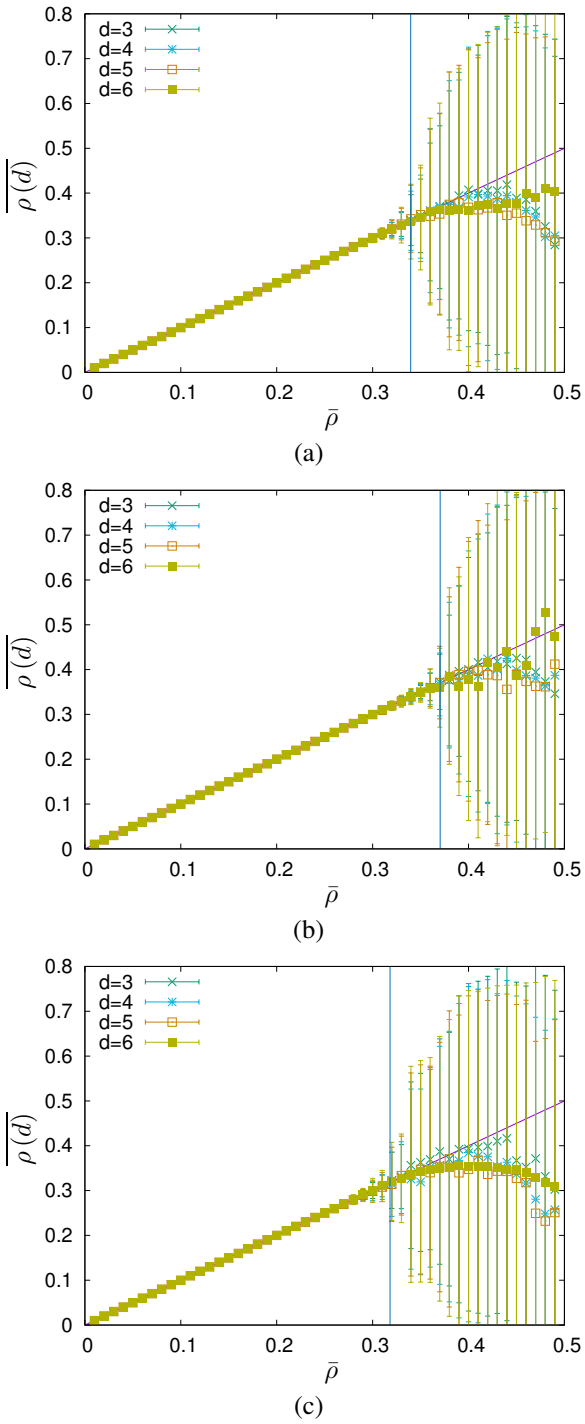

Fig. 2. Average and standard deviation of mean activities of nodes with degree d versus target activity $\bar{\rho}$. (a) $\lambda(3) = \lambda(4) = \lambda(5) = \lambda(6) = 0.25$, (b) $\lambda(3) = 0.7$, $\lambda(4) = \lambda(5) = \lambda(6) = 0.1$, and (c) $\lambda(3) = \lambda(4) = \lambda(5) = 0.1$, $\lambda(6) = 0.7$. The vertical line shows the local stability threshold, located at (a) $\bar{\rho} = 0.3397$, (b) 0.3704, and (c) 0.3182.

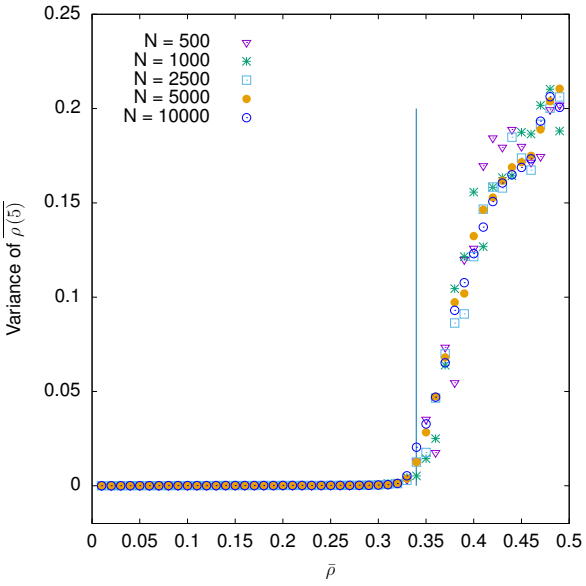

Fig. 3. Onset of phase transition in networks of varying sizes.

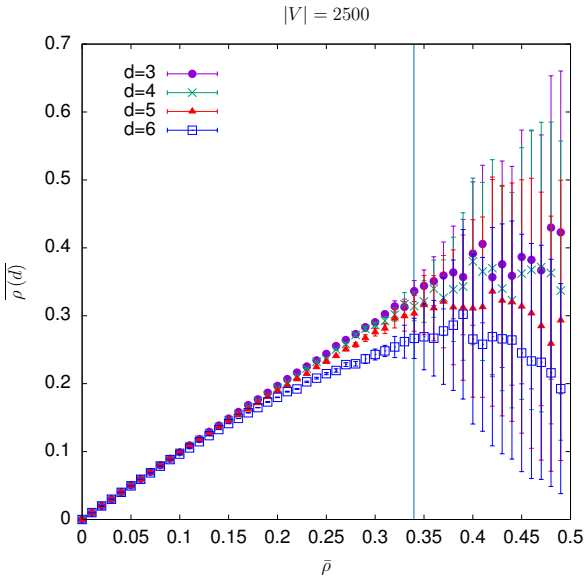

Fig. 4. Average and variance of mean activities of nodes in square grid networks with localized interference pattern.

activity $\bar{\rho}$ is not too high the proposed throughput equalization strategy works as expected. When the target activity $\bar{\rho}$ does not satisfy the local stability condition (14), on the other hand, we observe the onset of a phase transition where the variance in mean activities start to get very large, implying failure of the proposed throughput equalization strategy.

Figure 3 shows the results obtained by varying $|V|$ from 500 to 10 000, where the degree distribution was fixed to $\lambda(3) = \lambda(4) = \lambda(5) = \lambda(6) = 0.25$. The plot shows the variance of mean activities of nodes of degree 5 as a function of $\bar{\rho}$. The figure shows that the onset of the phase transition is indeed independent of network size.

B. Grid networks

Wireless networks are better modeled as geometric graphs where interference is localized. We next simulated networks where nodes are placed on square grid and the interference is limited to a node's neighborhood. Node degrees were assigned randomly as before. However, the conflict graphs were constructed by attaching neighboring nodes in the order of increasing distance until node degrees were satisfied. The performance of our throughput equalization strategy on a realization of such a graph is shown in Figure 4. The strategy, though developed on the basis of mean-field model, works well for a smaller, though comparable, range of $\bar{\rho}$. In Figure 4 as target activity, $\bar{\rho}$, is increased, the average equalized throughput for $d = 6$ starts to get smaller than the rest somewhat before the critical point. However, the rate of degradation remains small until phase transition occurs.

C. Poisson networks

Last we evaluated the proposed equalization strategy on networks where node placements are distributed according to spatial Poisson Point Process. This model has been used with

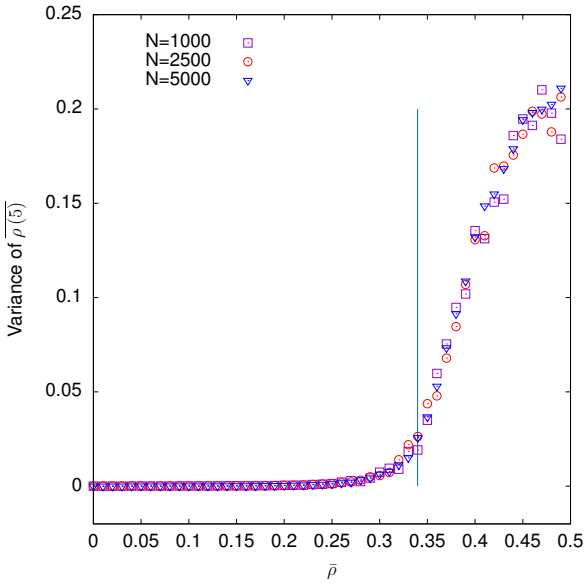

Fig. 5. Onset of phase transition in square grid networks of varying sizes.

significant interest by wireless ad-hoc networks and cellular networks research communities. We used the so-called disk model of interference where an active transmitter is detected during carrier sensing by nodes located within a specified radius from the transmitter. Figures 6–7 show the results of simulation where we deployed 500 Nodes in a field of size 1000m $\times$ 1000m with interference range of 125m. The network layout is shown in Figure 6, where the edges indicate interference. The average and variance of mean activities of nodes are shown in Figure 6. In the figure, we have plotted data for those degrees where $n_d \geq 10$. In contrast with the previous

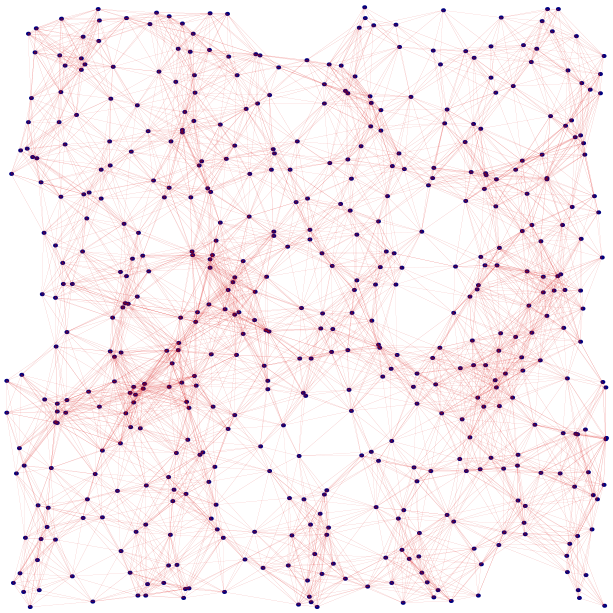

Fig. 6. Network layout

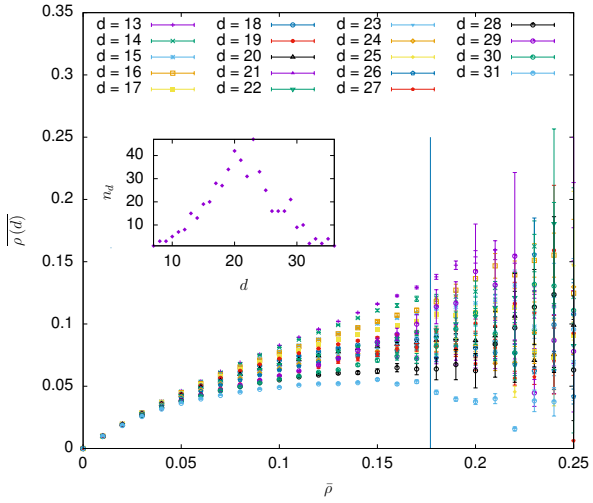

Fig. 7. Average and variance of mean activities of nodes in a network where nodes are placed according to spatial PPP along-with localized interference pattern.

evaluations, the range of degrees with non-trivial occupancy is much bigger. The figure shows that the proposed equalization strategy performs very well for low values of target activity $\bar{\rho}$. The average mean activity with hard-core interactions present starts to diverge as the target activity activity approaches the critical point. Till the critical point the variance too remains close to zero. The range of $\bar{\rho}$ where the average mean activity remains stable well covers the low data rate networks, such as, IEEE 802.15.4 networks. Furthermore, data rates higher than this is not sustainable even when nodes continuously try to access the medium (that is, back-off timer duration approaching 0), as we show later in this section.

We compared the average activity of nodes using our

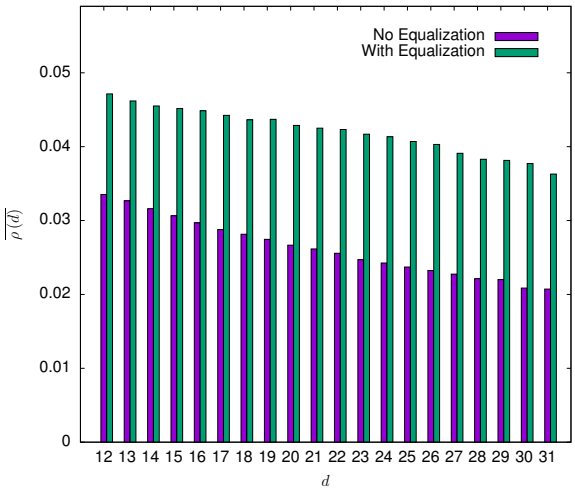

Fig. 8. Average mean activity. Parameter $\bar{\rho}$ was 0.05 for equalized channel access simulation and $e^{\mu_i} = 0.05\ \forall i$ for the case without equalization.

equalization strategy to that without it. Recall that in our equalization strategy, we set the transmission probability of node as a function of its degree, which is related to the target activity through (11). Figure 8 shows the comparison where we kept $\bar{\rho} = 0.05$ for the simulation where the equalization strategy was in place and $e^{\mu_i} = 0.05\ \forall i$ where we used CSMA without equalization. The network layout and simulation setting for this and the following figure was the same as stated earlier in this subsection. The simulation data shows that the proposed equalization strategy consistently gives higher mean activity, achieving 30–40% performance improvement.

The performance of the proposed equalization strategy gets better as we increase the target activity. We set $\bar{\rho}$ (for the equalized throughput simulation) as well as e^{μ_i} (for the non-equalized pure CSMA simulation) to 0.15. We also simulated the non-equalized pure CSMA case where the nodes are heavily contending to access medium by setting e^{μ_i} to 0.90. Figure 9 shows the comparison among all three scenarios. First of all, the efficacy of our equalization strategy is clearly visible. While the data for both scenarios without equalization show systematic decline in average throughput with increase in degree, such is not the case for the equalized channel access strategy. Second, for comparable target activity, the performance improvement given by the proposed equalization strategy increases to 100–200%. Third and perhaps the most interesting result is that for nodes having larger degrees (> 20 in this case) the average activity achieved by the proposed equalization strategy while keeping channel access probability low exceeds that of the case of non-equalized pure CSMA with high level of channel contention.

V. Discussion

Interference in networks of clusters of devices

Our analysis of the mean-field hard-core model can be extended to the case where each node in a conflict graph

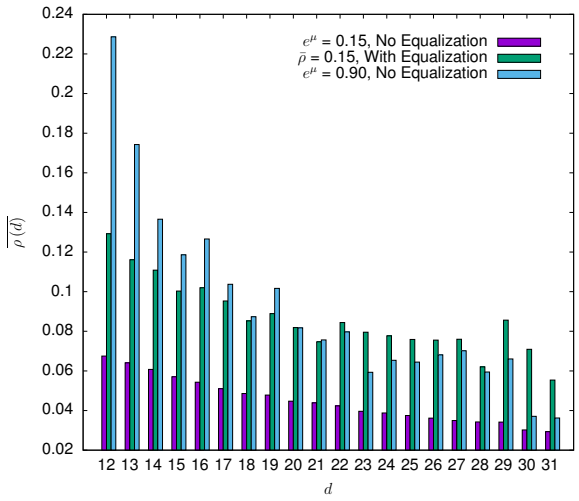

Fig. 9. Average and variance of mean activities of nodes in a network where nodes are placed according to spatial PPP along-with localized interference pattern.

corresponds not to a single wireless device but to a cluster of m distinct and mutually interfering devices. We show that analytical treatment of such an extension using the analytical framework developed earlier is possible under some assumptions, and that doing so yields results that contain several known results in the literature as special cases.

In the extended model mentioned above, at most one out of m devices in each cluster can be active at any time instance. Thus the state of a cluster is no longer a binary-valued variable but instead takes a value in $\{\mathbf{0}, \boldsymbol{e}_1, \ldots, \boldsymbol{e}_m\}$, where $\{\boldsymbol{e}_1, \ldots, \boldsymbol{e}_m\}$ is the standard basis of an m-dimensional space, with $\boldsymbol{e}_i$ representing the state that device i in the cluster is active (while the remaining $(m-1)$ devices are inactive). Accordingly, one needs m parameters to parametrize each message of belief propagation. If the clusters form a one-dimensional chain, then the model includes the linear network with $2m$ nearest-neighbor interactions discussed in [21], [28] as a special case, where it has been analytically shown that throughput equalization can be achieved by appropriately setting the intensity of each node on the basis of its degree. Their result can be reproduced within our framework since a one-dimensional chain is cycle-free, and belief propagation used in our work becomes exact when it is applied to trees, which includes one-dimensional chain as a special case.

In our extension we instead assume that inter-cluster interference is such that for any clusters $C, C' \subset V$ connected by an edge in the conflict graph, each device in cluster C interferes with exactly k devices in cluster C', and each device in cluster C' also does so exactly with k devices in cluster C, where $k \leq m$. So, k can be referred to as the number of inter-cluster interfering devices per edge. Then in the large-system limit, throughput equalization can be achieved by setting the intensities of devices in cluster C according to

$$\mu_C = \log \frac{\bar{\pi}}{(1-m\bar{\pi})(1-k\bar{\pi})^{|\partial C|-1}}, \tag{16}$$

where $|\partial C|$ is the degree of cluster C in the conflict graph, $\bar{\pi} \in [0, 1/m)$ is a parameter, and the target activity $\bar{\rho}$ is given by

$$\bar{\rho} = \frac{\bar{\pi}(1-k\bar{\pi})}{1-mk\bar{\pi}^2}. \tag{17}$$

Since the right-hand side of the above equation is monotonically non-decreasing in $\bar{\pi}$ when $\bar{\pi} \in [0, 1/m)$, one can determine $\bar{\pi}$ uniquely on the basis of the specified target activity $\bar{\rho}$. Noting that a device in cluster C has a within-cluster degree of $(m-1)$ and an inter-cluster degree of $|\partial C| \times k$, the above result shows that the intensity of a device in this setting can be appropriately determined on the basis of its degrees, irrespective of degrees of other devices, resulting in (once again) a local strategy to achieve throughput equalization. It should also be noted that by letting $k = m$, the above equations are reduced to (11) and (10), respectively, implying that the above result is indeed an extension of the analytical result obtained in Section III. Furthermore, specializing the above result to the case of a length-L linear network of clusters with $m = 2$ and $k = 1$ reproduces the result in [21] on the rectangular grid of size $2 \times L$.

VI. Conclusion

In this paper we introduced a mean-field model for interference in CSMA-based wireless networks. We developed a theory to address the problem of throughput equalization. We considered large-system limit in order to overcome the computational difficulty associated with computing the partition function. Based on this theory, we presented a distributed strategy for throughput equalization that uses local information only. We presented several results of Monte-Carlo simulations that confirm the effectiveness of the proposed strategy. We also showed that the limitations of the proposed strategy arise due to the onset of a certain phase transition. We discussed how the results of this work can be extended to equalize throughput in networks where nodes are clusters of devices in a decentralized way.

Acknowledgment

TT acknowledges support of the Grant-in-Aid for Scientific Research on Innovative Areas, MEXT, Japan (No. 25120008).

References

[1] D. Bertsekas and R. Gallager, *Data Networks (2nd ed.)*. Upper Saddle River, NJ, USA: Prentice-Hall, Inc., 1992.

[2] S. Keshav, *An Engineering Approach to Computer Networking: ATM Networks, the Internet, and the Telephone Network*. Boston, MA, USA: Addison-Wesley Longman Publishing Co., Inc., 1997.

[3] L. Kleinrock and F. Tobagi, "Packet switching in radio channels: Part I–carrier sense multiple-access modes and their throughput-delay characteristics," *IEEE Transactions on Communications*, vol. 23, no. 12, pp. 1400–1416, Dec. 1975.

[4] D. Stoyan, W. Kendall, and J. Mecke, *Stochastic Geometry and its Applications*, 2nd ed. Wiley, 1995.

[5] J. G. Andrews, R. K. Ganti, M. Haenggi, N. Jindal, and S. Weber, "A primer on spatial modeling and analysis in wireless networks," *IEEE Communications Magazine*, vol. 48, no. 11, pp. 156–163, Nov. 2010.

[6] M. Haenggi, *Stochastic Geometry for Wireless Networks*. Cambridge University Press, 2013.

[7] B. Matérn, *Spatial Variation*, 2nd ed., ser. Springer Lecture Notes in Statistics, 1986, vol. 36.

[8] F. Baccelli and B. Błaszczyszyn, *Stochastic Geometry and Wireless Networks: Volume I Theory*, ser. Foundations and Trends in Networking. Now Publishers, 2009, vol. 3, no. 3–4.

[9] ——, *Stochastic Geometry and Wireless Networks: Volume II Applications*, ser. Foundations and Trends in Networking. Now Publishers, 2010, vol. 4, no. 1–2.

[10] M. Haenggi, "Mean interference in hard-core wireless networks," *IEEE Communications Letters*, vol. 15, no. 8, pp. 792–794, Aug. 2011.

[11] H. ElSawy and E. Hossain, "A modified hard core point process for analysis of random CSMA wireless networks in general fading environments," *IEEE Transactions on Communications*, vol. 61, no. 4, pp. 1520–1534, Apr. 2013.

[12] B. Cho, K. Koufos, and R. Jäntti, "Bounding the mean interference in Matérn type II hard-core wireless networks," *IEEE Wireless Communications Letters*, vol. 2, no. 5, pp. 563–566, Oct. 2013.

[13] H. Nishimori, *Statistical Physics of Spin Glasses and Information Processing: An Introduction*. Oxford University Press, 2001.

[14] M. Mézard and A. Montanari, *Information, Physics, and Computation*. Oxford University Press, 2009.

[15] B. Bollobás, R. Kozma, and D. Miklós, *Handbook of Large-Scale Random Networks*. New York, NY, USA: Springer Publishing Company, Inc., 2009.

[16] Y. Kim, F. Baccelli, and G. de Veciana, "Spatial reuse and fairness of ad hoc networks with channel-aware CSMA protocols," *Information Theory, IEEE Transactions on*, vol. 60, no. 7, pp. 4139–4157, July 2014.

[17] P. M. van de Ven, S. C. Borst, J. S. H. van Leeuwaarden, and A. Proutière, "Insensitivity and stability of random-access networks," *Performance Evaluation*, vol. 67, no. 11, pp. 1230–1242, Nov. 2010.

[18] L. G. Valiant, "The complexity of enumeration and reliability problems," *SIAM Journal on Computing*, vol. 8, no. 3, pp. 410–421, August 1979.

[19] J. Pearl, *Probabilistic Reasoning in Intelligent Systems: Networks of Plausible Inference*. Morgan Kaufmann, 1988.

[20] T. Richardson and R. Urbanke, *Modern Coding Theory*. Cambridge University Press, 2008.

[21] P. M. van de Ven, S. C. Borst, D. Denteneer, A. J. E. M. Janssen, and J. S. H. van Leeuwaarden, "Equalizing throughputs in random-acceess networks," *ACM SIGMETRICS Performance Evaluation Review*, vol. 38, no. 2, pp. 39–41, Sept. 2010.

[22] J. Barbier, F. Krzakala, L. Zdeborová, and P. Zhang, "The hard-core model on random graphs revisited," *Journal of Physics: Conference Series*, vol. 473, no. 012021, 2013.

[23] F. Krzakala, C. Moore, E. Mossel, J. Neeman, A. Sly, L. Zdeborová, and P. Zhang, "Spectral redemption in clustering sparse networks," *Proceedings of the National Academy of Sciences of the United States of America*, vol. 110, no. 52, pp. 20 935–20 940, Dec. 2013.

[24] Z. Király, "Recognizing graphic degree sequences and generating all realizations," Eötvös Loránd University, Tech. Rep. Egres TR-2011-11, 2012.

[25] A. Iványi, L. Lucz, T. F. Móri, and P. Sótér, "On Erdös-Gallai and Havel-Hakimi algorithms," *eprint arXiv*, vol. 1111.3282, 2011. [Online]. Available: http://arxiv.org/abs/1111.3282

[26] J. Blitzstein and P. Diaconis, "A sequential importance sampling algorithm for generating random graphs with prescribed degrees," *Internet Mathematics*, vol. 6, no. 4, pp. 489–522, 2010.

[27] C. I. D. Genio, H. Kim, Z. Toroczkai, and K. E. Bassler, "Efficient and exact sampling of simple graphs with given arbitrary degree sequence," *PLoS ONE*, vol. 5, no. 4, p. 7 pages, April 2010.

[28] P. M. van de Ven, A. J. E. M. Janssen, J. S. H. van Leeuwaarden, and S. C. Borst, "Achieving target throughputs in random-access networks," *Performance Evaluation*, vol. 68, no. 11, pp. 1103–1117, Nov. 2011.